PHILOSOPHICAL TRANSACTIONS OF THE ROYAL SOCIETY A MATHEMATICAL, PHYSICAL & ENGINEERING SCIENCES

Results of an Experimental Investigation of Correlations between D-Region Neutral Gas Winds, Density Changes and Short-Wave Radio-Wave Absorption [and Discussion]

G. Rose, H. U. Widdel, A. Azcarraga, L. Sanchez and R. A. Hamilton

Phil. Trans. R. Soc. Lond. A 1972 **271**, 529-545
doi: 10.1098/rsta.1972.0021

Phil. Trans. R. Soc. Lond. A. **271**, 529–545 (1972) [529]
Printed in Great Britain

Results of an experimental investigation of correlations between D-region neutral gas winds, density changes and short-wave radio-wave absorption

By G. Rose and H. U. Widdel
Max-Planck-Institut für Aeronomie, D-3411 *Lindau/Harz*,
Federal Republic of Germany

and A. Azcárraga and L. Sanchez
Instituto Nacional de Técnica Aeroespacial, *Torrejon de Ardoz*, *Spain*

Between December 1969 and March 1970 a total of 26 Skua II rockets were successfully launched close to local noon at Arenosillo, Spain. Using an ultralight chaff the winds and chaff fall rates have been determined at heights between 75 and 95 km. At the same time A_3-absorption measurements were carried out on 2.83 MHz between Aranjuez (Madrid) and Arenosillo.

From the wind and fall-rate measurements a quantity which is roughly proportional to the air mass flow has been derived for each km height range. These flow vectors were obtained on different days at different height levels and correlated with the noon absorption values $L \sim \int N\nu \, dh$ which were taken from the short-wave propagation path between Arenosillo and Aranjuez.

A significant but not very high correlation was found between the mass flow at 90 to 93 km and the absorption L, with L increasing with increased flow from the north-northeast, and at 85 km with L increasing with increased flow from the south-southwest. For the other heights between 75 and 95 km a significant correlation could not be found although there is some indication at 77 km.

1. Introduction

During the last years it has become clear that seasonal variations in the D region probably involve the atmospheric circulation (Dieminger 1952) and the photochemistry of minor constituents (Bowhill 1969; Gregory & Manson 1969). This seems to be particularly true for any explanation of the winter anomaly of radio-wave absorption (Manson 1971), because the Sun's ionizing radiation is not normally found to be stronger on anomalous days than on others. Sudden changes from periods of rather high to very low absorption, which have been observed very distinctly in winter on our field-strength records obtained in Sardinia (Dieminger, Rose & Widdel 1966; Weber 1967) and in Spain (Rose, Schubart, Weber, Widdel & Galdron 1971), also indicate the presence of large-scale transport phenomena.

In this paper some of the results obtained from our simultaneous measurements of D-region winds and radio-wave absorption are given.

2. Chaff fall rates and diurnal atmospheric variations

Winds have been measured with a special chaff released close to the apogee of Skua II rockets in the form of spherical chaff clouds consisting of a great number (approx. 6×10^4) of ultralight aluminized Hostaphan dipoles, which can be followed by a suitable radar. Differing from the needle type of chaff, commonly used by meteorologists to explore the winds at heights well below 70 km, the chaff we used was cut from foil bands to a size of 9×50 mm which corresponds to half the operational wavelength of the MPS 19 S-band radar set. The chaff foils were 2.5 μm

FIGURE 1. Location of Arenosillo and of the Aranjuez–Arenosillo transmission line ($f = 2.83$ MHz, mid-point at $\phi = 38.58°$ N; $\lambda = 5.21°$ W).

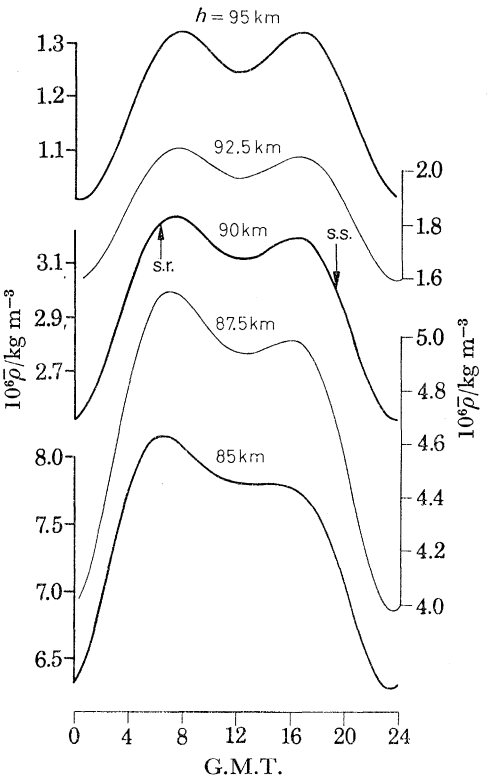

FIGURE 2. Variation of mean air density over Arenosillo after chaff fall rates of 24 to 28 February 1970 and C.I.R.A. Standard Atmosphere. The Fourier-synthesized $\rho(h)$ curves are based on mean exponential fall rates obtained from measurements at 0, 4, 8, 12, 16 and 20 G.M.T., see appendix C.

thick and their wing loading was only 3.5 g/m². With this type of chaff the fall rates have been about 80 m/s at a height of 95 km and about 10 m/s at 80 km. It is not possible to give more technical details here (Rose *et al.* 1972, this volume).

In our combined wind and absorption programme, which was carried out between December 1969 and the beginning of March 1970, a total of 26 Skua II rockets were successfully launched close to local noon at Arenosillo, Spain; at the same time a 2.83 MHz wave was transmitted from Aranjuez near Madrid to Arenosillo. From the field-strength records radio wave absorption was determined by using the well-known A_3 method. Figure 1 shows the locations of Arenosillo and of the A_3 transmission line.

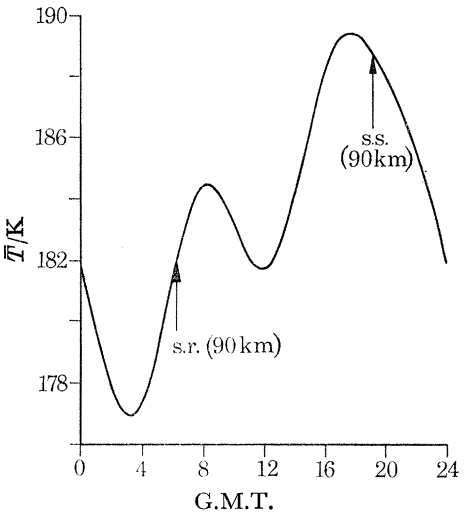

FIGURE 3. Mean air temperature variation between 83 and 95 km (24 to 28 February 1970) over Arenosillo as derived from the mean scale-heights of the chaff fall rates: see also caption of figure 2.

If it is true, that minor constituents, which are considered necessary to produce a winter anomaly, are transported by D-region winds, there should be a significant correlation between air mass flow and D-layer absorption in winter. Now a quantity which is approximately proportional to the air mass flow at a given height level in the D region is obtained by the simple expression: wind velocity divided by chaff fall rate, the latter being roughly inversely proportional to air density. It should be mentioned that in our measurements, chaff fall rates are not influenced too much by turbulence above a certain height level. This can be shown by evaluating density variations above about 83 km from them. Figure 2 shows such an evaluation obtained from the fall for a 4-day launching period during which measurements were made every 4 h. It is seen that a rather regular mean daily air density variation comes out. The evaluation procedure is based on a calibration of the chaff fall rates with the aid of C.I.R.A. 1965. From the scale heights of the chaff fall rates between 85 and 95 km mean temperature variations have been deduced, which are shown in figure 3.

3. CORRELATIONS BETWEEN WINDS AND RADIO-WAVE ABSORPTION

In order to search for correlations between air mass flow and radio-wave absorption, the flow vectors (obtained between 75 and 95 km at local noon on the different days) have been associated with the corresponding noon absorption values for each kilometre of height. Because we did not

measure absorption as a function of height but as the integral noon absorption along the Aranjuez–Arenosillo transmission line, the same set of absorption data has been used repeatedly to be correlated with the accompanying wind data from different heights. With this procedure it is evident that no surprisingly high correlations are to be expected, because different effects at different heights may partly cancel each other. Therefore *t*-statistics have been applied for the purposes of testing whether a significant correlation is likely to exist or not.

Figures 4 and 5 show the results obtained from the calculations. On the left of these diagrams the sums of all wind velocities measured at noon from the different directions at the relevant height

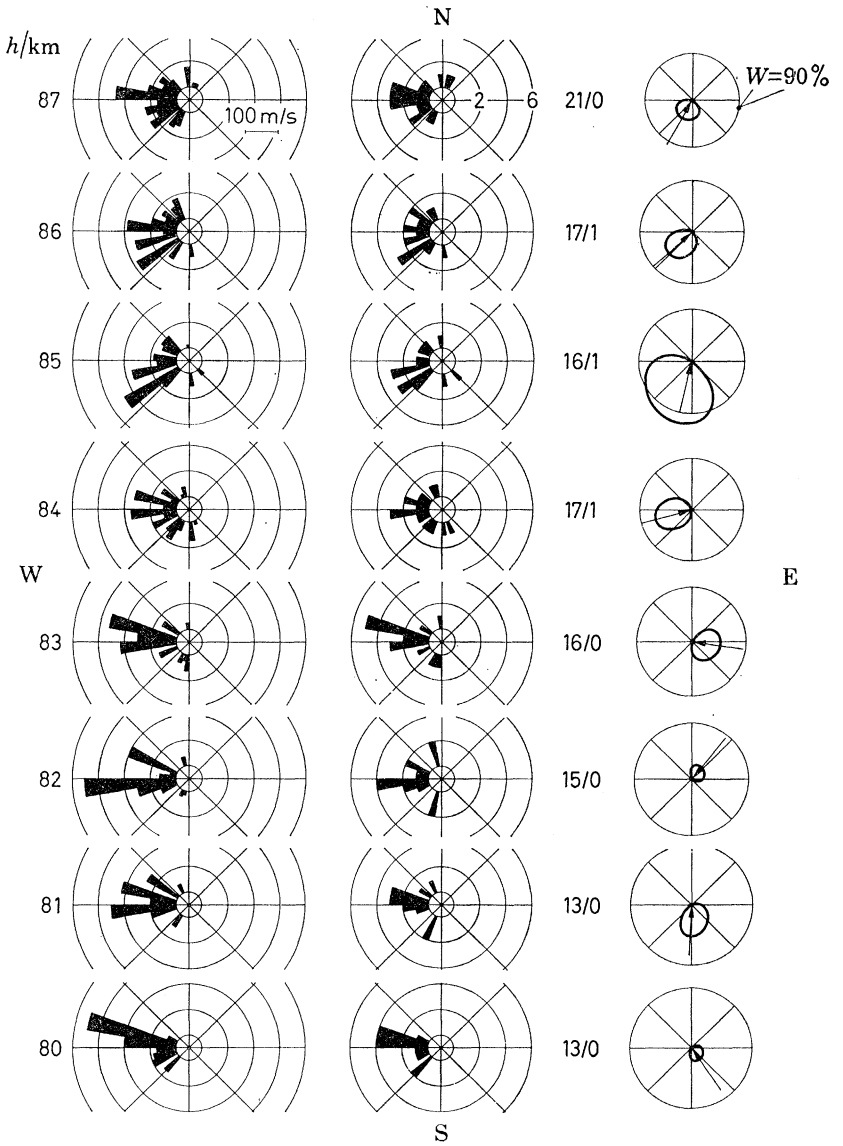

FIGURE 4. On the left: sums of all wind speeds measured at noon over Arenosillo between December 1969 and the beginning of March 1970 with a total of 26 wind-finding rockets; the directions from which the winds came are indicated (10°-intervals). Central part: total number of wind observations obtained from the different directions at the relevant heights, the numbers of observed calms are quoted behind the dashes. On the right: beam diagrams of the correlation coefficients between radio-wave absorption $\bar{L}_{\mathrm{M}}\left(\sim \int N\nu \,\mathrm{d}h\right)$ measured at noon (11h00 to 13h00 G.M.T.) on the different days and the accompanying air mass-flow components from different points of the compass. The circles around each of these diagrams quote the 90% probabilities of $w(n, r)$; see also appendixes A and B.

levels are drawn. In the centre, the corresponding numbers of measurements are given for the relevant direction sectors. The total number of wind observations at the relevant heights are indicated by the first digits, the second digit indicates the number of calms observed. On the right,

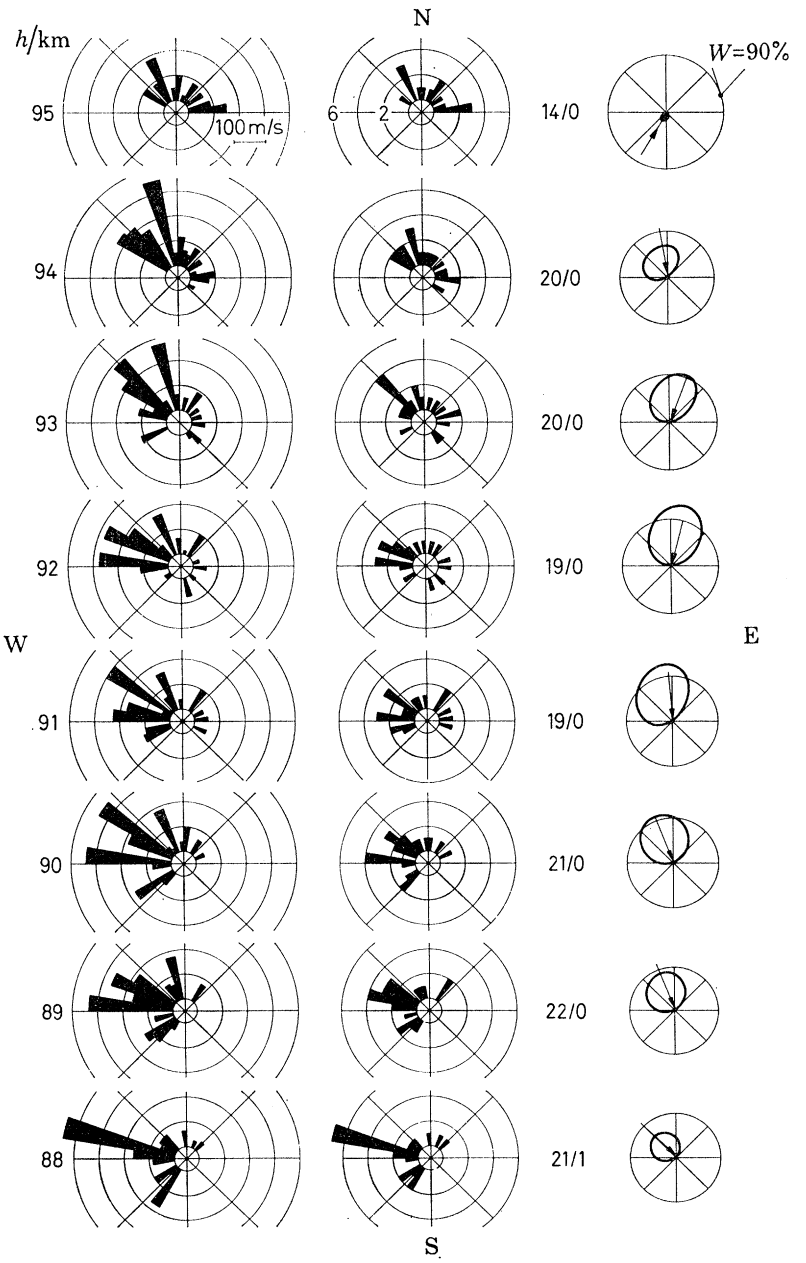

FIGURE 5. See text of figure 4.

beam diagrams of the correlation coefficients obtained from the correlation calculations between the flow vectors at the different height levels and the ground-based absorption measurements are drawn. These beam diagrams have been obtained in principle by resolving all the measured flow vectors at the different heights into components around the compass and then correlating all these components with the corresponding absorption data successively. The beam diagrams now

show up the directions from which, on the average, an air mass flow has produced the most significant increase of absorption during our measurements.

The circles drawn around each of these diagrams indicate the 90 % probabilities $w(n, r)$, where n is the number of data points and r the correlation coefficient, that the absolute value of a correlation coefficient calculated from n pairs of random numbers is smaller than that one represented by the corresponding circle; see appendix A.

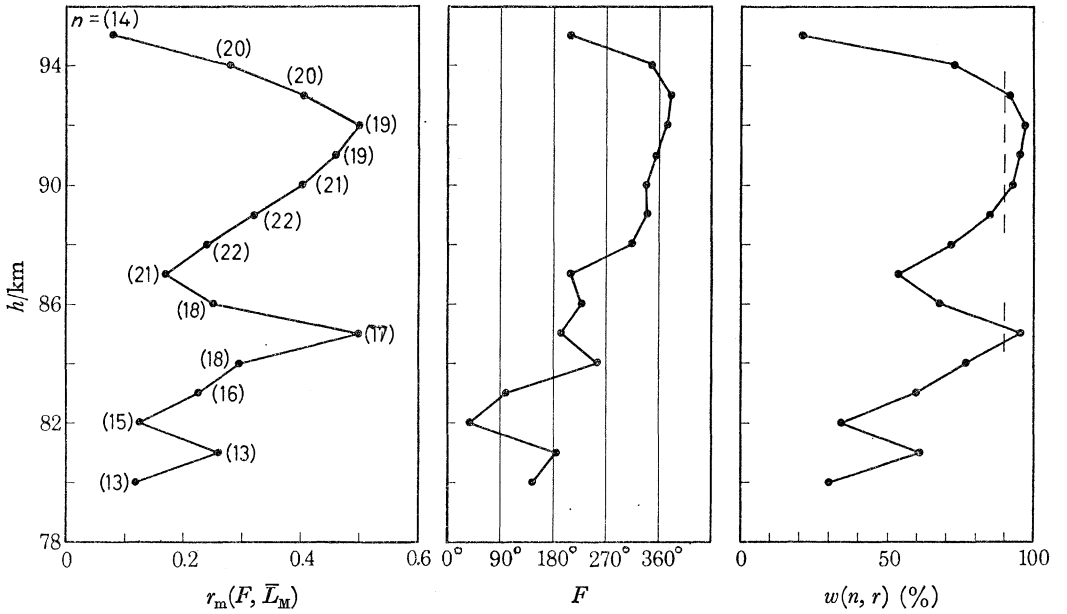

FIGURE 6. On the left: correlation coefficients $r_m(F, \bar{L}_M)$ between radio-wave absorption $\left(L_M \sim \int N\nu \, dh\right)$ measured at noon (11h00 to 13h00 G.M.T.) on different days and the accompanying air mass flow components F from the directions of maximum correlation coefficients, which are shown in the centre of this figure. On the right: The corresponding $w(n, r)$ values, see also appendix A.

It can be seen that correlations between winds and radio-wave absorption which are more than 90 % reliable were found at 85 km and between 90 and 93 km. Absorption increased with increasing winds from southern directions at 85 km and with increasing winds from northern directions between 90 and 93 km.

Figure 6 shows the same results in a little different way. The correlation coefficients as a function of height are shown on the left in this diagram, the corresponding directions of flow are to be found in the centre and the probabilities for having a genuine correlation between air mass flow at the different heights and absorption are drawn on the right.

4. Other correlations

In order to check if the height levels around 85 km and between 90 and 93 km are still of importance when other parameters which can be deduced from the wind and absorption measurements are brought into play, correlation calculations have also been performed with the following parameters:

(1) Meridional wind components and absorption.

(2) Air density derived from the chaff fall rates and absorption.

Further, two other parameters have been deduced from the daily variations of absorption L. The exponents n in the equation $L = L_0 \cos^n \chi$ have been calculated from the L values measured between morning and noon on the individual days and the corresponding solar zenith angles χ

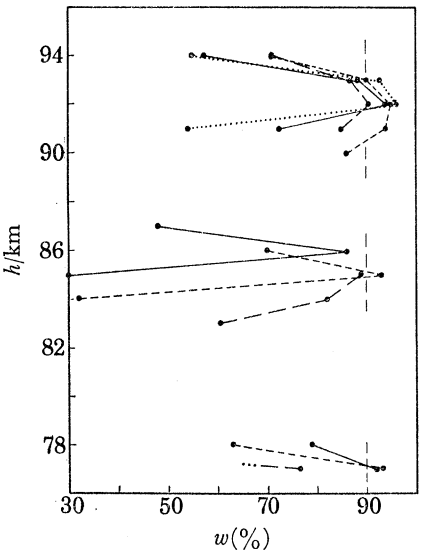

FIGURE 7. Probabilities $w(n, r)$ obtained from correlation calculations: ····, between the meridional wind components v_{NS} and the absorption parameter r_S (see text); —, between v_{NS} and the exponents n (in $L = L_0 \cos^n \chi$); — —, between air-density ρ and noon absorption L_M; and, – – –, between v_{NS} and L_M.

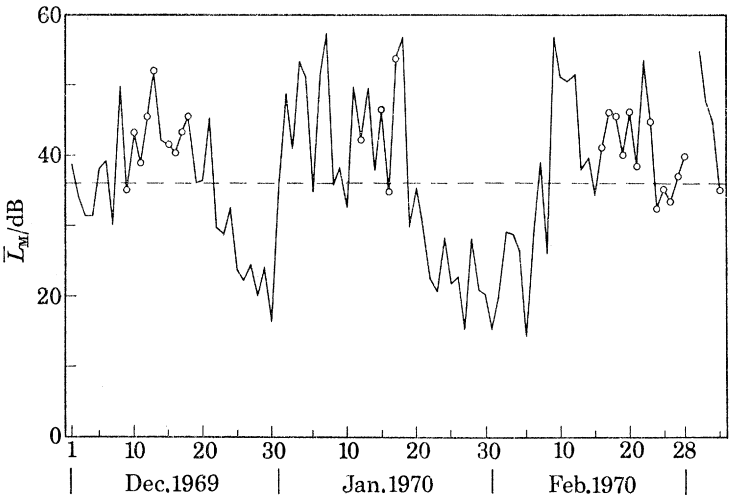

FIGURE 8. Daily noon absorption $\bar{L}_M$ (11h00 to 13h00 G.M.T.), obtained from the Aranjuez–Arenosillo transmission line ($f = 2.83$ MHz). The days of successful wind-finding launchings at noon are indicated by small circles. The dashed horizontal line indicates the average 'no wind' (or 'no flow') condition obtained from figure 9.

at the centre of the transmission path. A quatity r_S measuring the goodness of fit of the absorption values L to the $\cos^n \chi$-law has been derived. With these two quantities:

(3) The exponent n and the quantity r_S have been correlated with the meridional wind components.

The results of the additional correlation calculations are shown in figure 7. The above-mentioned probabilities are shown as a function of height and indicate that the correlations are

probably genuine around 85 km and still more probably around 92 km. Some indication is obtained from heights as low as 77 km, but more measurements are required to decide whether these correlations are genuine or not.

Figure 8 shows the daily noon absorption values which were obtained from the Aranjuez–Arenosillo transmission path between December 1969 and the beginning of March 1970. The days of successful launchings are indicated in the diagram with small circles. As can be seen, nearly

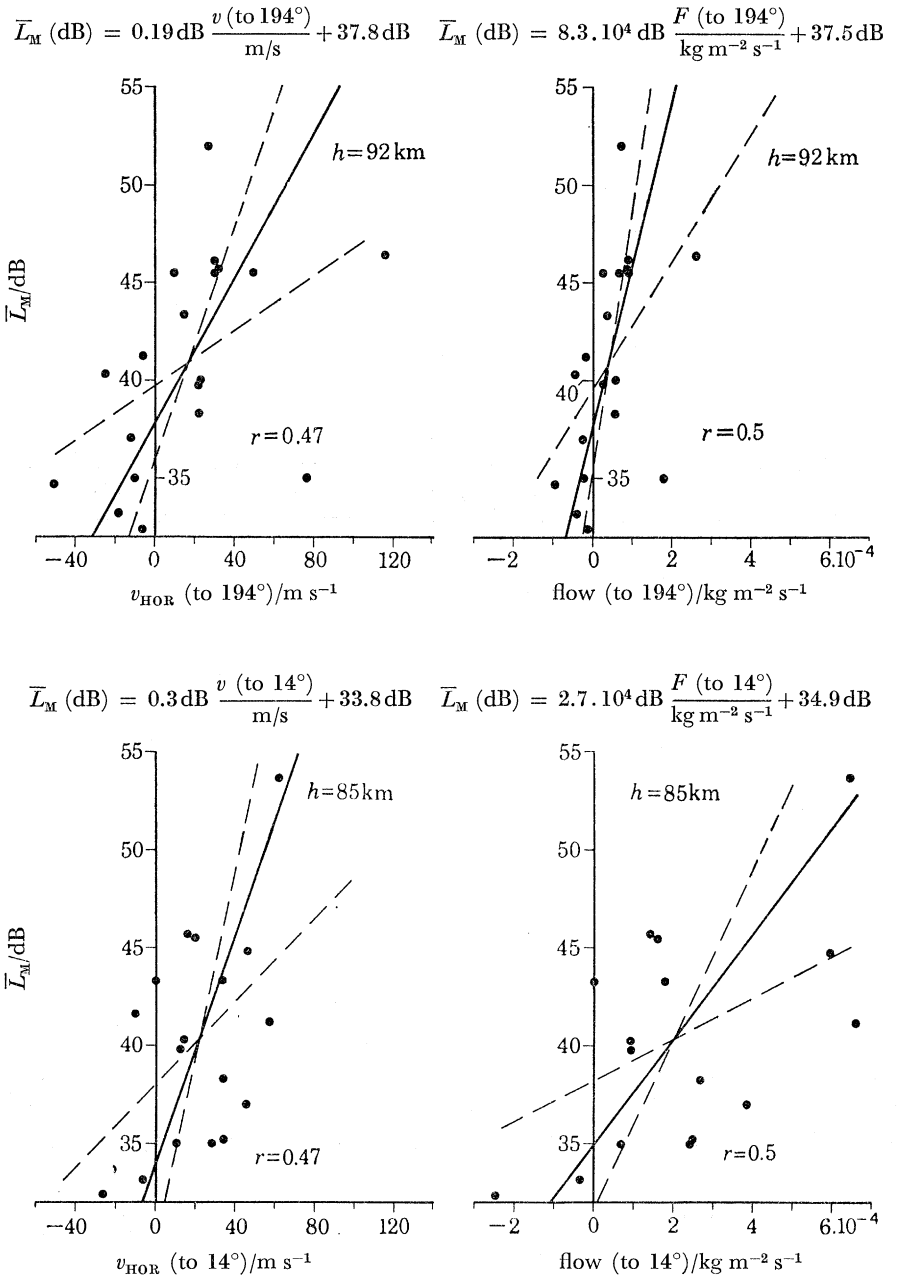

FIGURE 9. Correlograms between the wind components (air mass flow components) at local noon to the directions of maximum correlation and the accompanying radio-wave absorption $\bar{L}_M$. The dashed lines are obtained by minimizing the sums of the squares of the horizontal or vertical distances of the data points from the corresponding dashed lines. The thick lines are the resulting averages between these, the equations of which are indicated; see also appendix C.

all wind-finding rockets were flown under fully developed winter-anomalous conditions. This was not intended initially but came about as a matter of chance when weather conditions and technical reasons prevented firings during the periods of lower absorption. It is therefore probable that

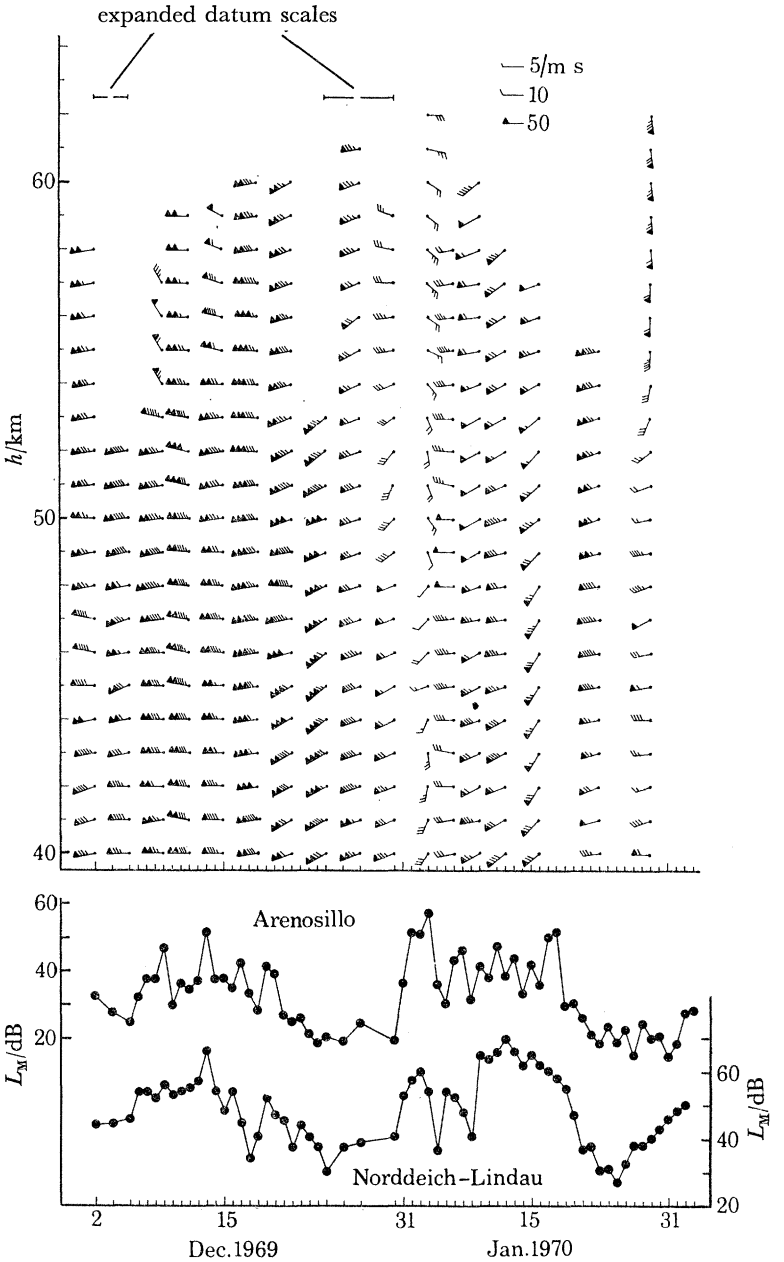

FIGURE 10. Winds over South Uist (Hebrides) and the accompanying noon absorption of the Norddeich–Lindau (Germany) and of the Aranjuez–Arenosillo (Spain) transmission lines. We wish to express our thanks to the colleagues of the British Meteorological Office from whom we obtained the wind data represented here.

we would have obtained still higher correlation coefficients if we had had firings under conditions of low absorption too. This is also supported by the plots of figure 9 for the main correlograms between winds and absorption as well as between air mass-flow and absorption: all the point clouds there would probably have been elongated with measurements under low absorption conditions.

The two dashed lines drawn in each plot of figure 9 represent the linear regressions determined by minimizing the sums of the squares of the horizontal or vertical distances of the data points from the corresponding dashed lines respectively. The thick line in each plot is the resulting average between the two least mean-square lines. These thick lines intersect the ordinates in each of the four plots at slightly different absorption values for average no flow or no wind conditions. The mean of these 'no wind' (or 'no flow') absorption values has been represented as a dotted line in figure 8. It divides the measured absorption values into groups of high and low absorption.

Finally it should be mentioned that remarkable changes of the winds as being observed well below 65 km over South Uist (Hebrides) have been associated with significant changes of radio wave absorption in Europe. This is clearly demonstrated by figure 10 in which the daily winds over South Uist are represented together with the accompanying radio wave absorption which has been measured at noon in Spain and Germany.

5. Conclusion

Summarizing the results of our measurements it can be said that days of anomalous winter absorption are associated with D-region wind phenomena. In Spain absorption increased in winter with increasing air mass flow (or wind) components from northern directions between 90 and 93 km and with increasing mass flows (or winds) from southern directions at 85 km.

The German part of this cooperative programme was made possible with a research grant from the Bundesminister für Bildung und Wissenschaft (Projekt WRK 90) for which we express our sincere thanks.

Appendix A. Determination of $w(n, r)$

When a correlation coefficient r is calculated from a set of n pairs of numbers chosen arbitrarily from among the real numbers, r tends to zero as n increases indefinitely. If, on the contrary, n is finite the coefficients obtained thus by chance are distributed in between -1 and $+1$ with a maximum density at $r = 0$ (if $n > 4$). With an increasing number n of points (pairs of random numbers) the concentration of r at $r = 0$ increases.

In order to find out if a significant correlation exists between two physical parameters, which are represented by a small sample of experimental points, it is necessary to consider the calculated correlation coefficient r and the number of data points as well. This is normally done by applying t-statistics (see, for example, *Statistics in research*, B. Ostle, Iowa State Press 1966). An equivalent derivation, which leads to the same results, has been applied here; it will be outlined briefly.

The density distribution functions $d_n(r)$ of correlation coefficients calculated from n pairs of random numbers $x_1 y_1$, $x_2 y_2$,..., $x_n y_n$ are first required. These can be obtained if one considers a correlation coefficient an equivalent to the scalar product of the two associated n-dimensional unit vectors $(\tilde{x}_1, \tilde{x}_2, \ldots, \tilde{x}_n)$ and $(\tilde{y}_1, \tilde{y}_2, \ldots, \tilde{y}_n)$ with the sums of their components being zero, that is $\Sigma\tilde{x}_\nu = \Sigma\tilde{y}_\nu = 0$.

For the case $n = 3$, each of the two associated three-dimensional unit vectors must lie on the surface of the same unit sphere around the origin. Furthermore, as the sum of the components of each of the two vectors is zero, they must be located in the same plane through the origin,

defined by $\Sigma x_\nu = 0$ (or, what is equivalent, by $\Sigma y_\nu = 0$). That is, they define the same great circle on the surface of the unit sphere on which their points are distributed with equal probability because of the symmetry of the problem. If n increases now, the problem is successively transferred into higher dimensions, where the points of the corresponding two n-dimensional vectors are distributed with equal probabilities on the surfaces of $(n-1)$-dimensional unit spheres around the origin.

From this geometrical picture, it is easy to obtain the before-mentioned density distribution functions $d_n(r)$. They are

$$d_n(r) = \frac{(1-r^2)^{\frac{1}{2}(n-4)}}{\int_{-1}^{+1} (1-r^2)^{\frac{1}{2}(n-4)}\,\mathrm{d}r} \qquad (n \geqslant 3,\ |r| \leqslant 1),$$

with

$$\int_{-1}^{+1} d_n(r)\,\mathrm{d}r = 1.$$

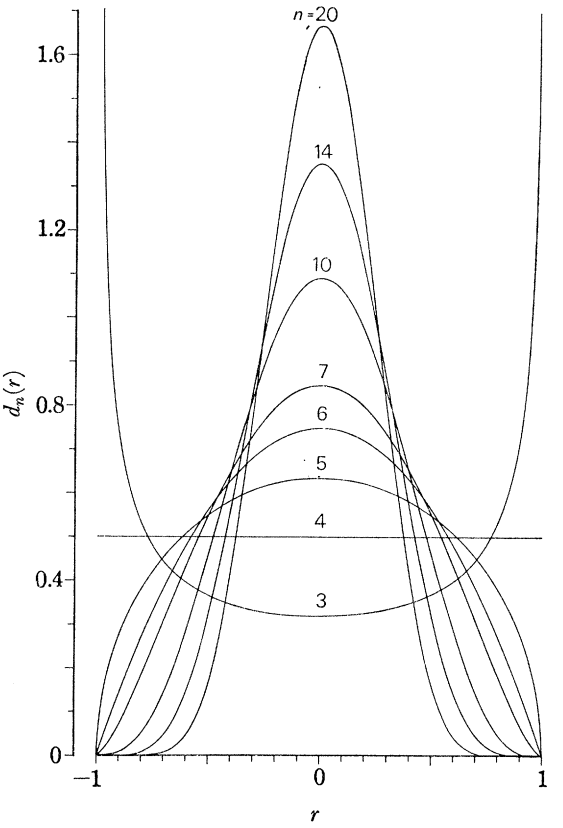

FIGURE 11. Some density distribution functions $d_n(r)$.

Some of these functions are illustrated by figure 11. Now, with the aid of these density distribution functions, we obtain the probabilities:

$$w(n, |r_0|) = 2\int_0^{|r_0|} d_n(r)\,\mathrm{d}r.$$

Suppose a correlation coefficient r_0 has been calculated for a set of n experimental data points. If now the correlation coefficient r of an equal number n of random points is determined, then $w(n, |r_0|)$ is the probability that the absolute value $|r|$ of such a random correlation coefficient

is smaller than $|r_0|$. If $w(n, |r_0|)$ is very close to unity, for example, then it is highly probable, that r_0, belonging to the experimental parameters, indicates a significant correlation between them.

For practical handling, the series expansion of $w(n, r)$ are:

$n \geqslant 3$, *odd*:

$$w(n,r) = \frac{2}{\pi}\left[\arcsin r + (1-r^2)^{\frac{1}{2}} r + \tfrac{2}{3}(1-r^2)^{\frac{3}{2}} r + \frac{2\times 4}{3\times 5}(1-r^2)^{\frac{5}{2}} \times r + \ldots + \frac{2\times 4\times 6\ldots(n-5)}{3\times 5\times 7\ldots(n-4)}(1-r^2)^{\frac{1}{2}(n-4)} r\right],$$

$n \geqslant 4$, *even*:

$$w(n,r) = r\left[1 + \tfrac{1}{2}(1-r^2) + \frac{1\times 3}{2\times 4}(1-r^2)^2 + \ldots + \frac{1\times 3\times 5\ldots(n-5)}{2\times 4\times 6\ldots(n-4)}(1-r^2)^{\frac{1}{2}(n-4)}\right].$$

Appendix B. The determination of beam diagrams of correlation coefficients and the estimation of their accuracies with the aid of model calculations

In the following we designate the meridional wind components by M_i, the accompanying zonal component by Z_i (M_i is positive for winds going to the north, Z_i for winds going to the east) and the absorption values which were measured at the same time by y_i. The correlation coefficient $r(\alpha)$ between the wind components going towards the direction α (α being measured clockwise from the north) and the absorption values is then described by

$$r(\alpha) = \frac{A\cos\alpha + B\sin\alpha}{\sqrt{(C\cos^2\alpha + D\sin^2\alpha + 2E\sin\alpha\cos\alpha)}}\,\frac{1}{\sqrt{F}},$$

with

$$A = \Sigma M_i y_i - (1/n)\,\Sigma M_i\,\Sigma y_i, \qquad D = \Sigma Z_i^2 - (1/n)\,(\Sigma Z_i)^2,$$
$$B = \Sigma Z_i y_i - (1/n)\,\Sigma Z_i\,\Sigma y_i, \qquad E = \Sigma M_i Z_i - (1/n)\,\Sigma M_i\,\Sigma Z_i,$$
$$C = \Sigma M_i - (1/n)\,(\Sigma M_i)^2, \qquad F = \Sigma y_i^2 - (1/n)\,(\Sigma y_i)^2.$$

In figures 4, 5 and 12, which show the results of experimental and model calculations, the correlation coefficients $r(\alpha)$ were based on the directions *from* which the winds came.

In order to obtain an estimate of the accuracy of this correlating procedure the following model calculations have been performed. With the aid of random numbers 20 'winds' of different amplitudes and from different directions were synthesized. Appropriate to the winds thus obtained the quantities y_i corresponding to the absorption values were calculated in the following way: at first, the vector component of each 'wind' in a given direction was determined, then the y_i 'absorption' values were calculated in such a way that they were proportional to the corresponding wind components W_i of that direction.

With these 'wind' and 'absorption' values it is clear that the correlation coefficient $r(\alpha)$ must reach a maximum of unity for the given direction. To each of the y_i values random numbers of small maximum amplitude were added and the beam diagram was calculated; then the same procedure was repeated with a somewhat higher maximum amplitude of the random numbers and so on. In this way, the maximum correlation coefficient was decreased successively. (Instead of just the y_i values, the winds or both could have been subjected to random fluctuations.)

The results of such model calculations are demonstrated by figure 12. The 20 'winds' of these

diagrams have been chosen from different points of the compass, which are indicated by the thick circular arcs at the periphery of each diagram. The initial directions of maximum correlations are shown up by arrows there. It can be seen from figure 12 that the initially adopted directions are again found with surprisingly good accuracies even if the maximum correlation coefficients are no longer close to unity.

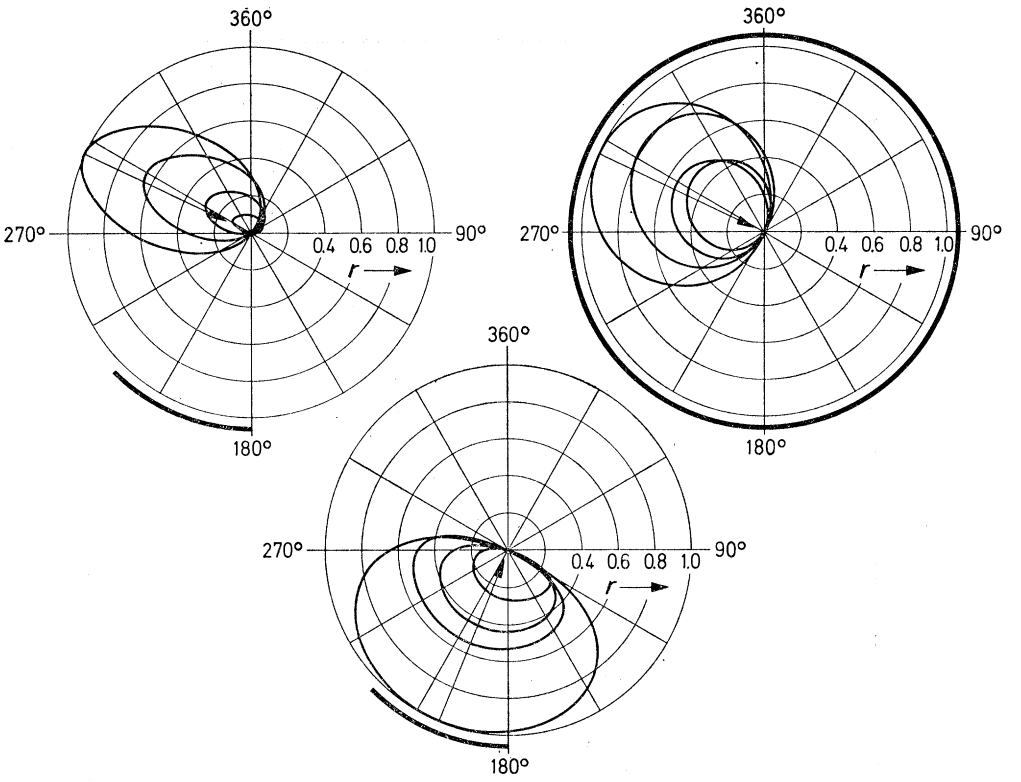

FIGURE 12. Three different model beam diagrams of correlation coefficients each of which was obtained from 20 triplets (M_i, Z_i, y_i) of synthesized 'wind' and 'absorption' parameters; see appendix B.

APPENDIX C. THE DETERMINATION OF DENSITY CHANGES FROM THE CHAFF FALL-RATES

In order to calculate air densities $\rho(h)$ from the fall rates $v_\perp(h)$ of the chaff clouds, which have been measured experimentally, it is necessary to know their drag coefficients c_w as a function of the Reynolds number $Re = \rho v l/\eta$. Then the differential equation of motion

$$m\dot{v} = -mg + \tfrac{1}{2}c_w \rho F v^2$$

can be solved numerically to obtain $\rho(h)$.

As $c_w(Re)$ is not known for D-region heights, another procedure was used to obtain information about the (relative) density variations there.

Now, for the height region between about 83 and 95 km it was found that, on the average, $v(h)$ (see figure 13) was as near to an exponential function of height ($v_\perp \approx v_{\perp 0}\, e^{+h/\overline{H}_v}$) as were the C.I.R.A. 1965 $\rho(h)$ values ($\rho \approx \rho_0\, e^{-h/\overline{H}_\rho}$) with the difference, that the scale height of $\bar{v}_\perp(h)$ was approximately 1.3 times the scale height of ρ. This was found by comparing with C.I.R.A. the average fall rates $v_\perp(h)$ obtained from a 4-day launching period, during which

every 4 h wind-finding measurements were made. A factor of 1.3 is not possible if c_w is a constant, in which case $\bar{H}_v/\bar{H}_\rho$ should be about 2 under equilibrium conditions, that is, when $mg \approx \frac{1}{2}c_w\rho Fv^2$.

In our case an approximation of c_w should have the form

$$c_w \approx C\rho^\gamma v^\theta,$$

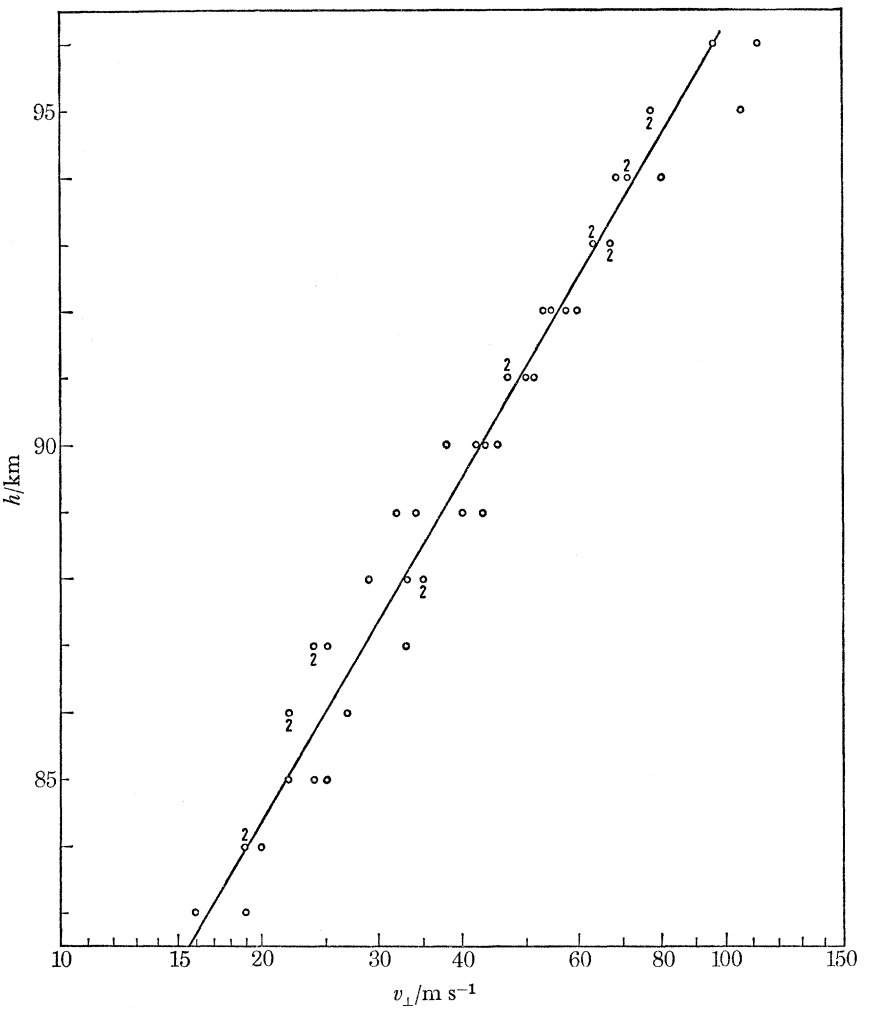

FIGURE 13. Fall rates obtained from the 20h00 G.M.T. launchings in February 1970 at Arenosillo.

which follows, when we again consider the equilibrium case. Further, if $\bar{H}_v/\bar{H}_\rho$ is known, the relation between the exponents γ and θ in c_w must be

$$\frac{2+\theta}{1+\gamma} = \bar{H}_v/\bar{H}_\rho.$$

All γ and θ values satisfying this equation, approximate the observations in the equilibrium case if for a given pair of γ and θ the constant C is appropriately chosen.

Although only one of these c_w functions is the correct one. But it is not necessary to know this as long as only fall rates under equilibrium conditions are considered. On the other hand, the true drag coefficient is of importance if the 'time constant' of the chaff cloud in the horizontal

winds is required. This can now be obtained on a half-empirical basis if one considers the behaviour of the drag-coefficients of similar bodies at small Reynolds numbers (Hoerner 1965). On the basis of such considerations the 'true' mean drag-coefficient c_w of our chaff clouds between about 83 and 95 km was estimated to be about

$$c_w = 25.3\ (\rho[\mathrm{kg\ m^{-3}}])^{-0.24}\ (v[\mathrm{m\ s^{-1}}])^{-1}. \tag{1}$$

Figure 14 shows the behaviour of our chaff clouds in horizontal winds at different heights. It is assumed that at $t = 0$ the falling cloud has no horizontal velocity component with respect

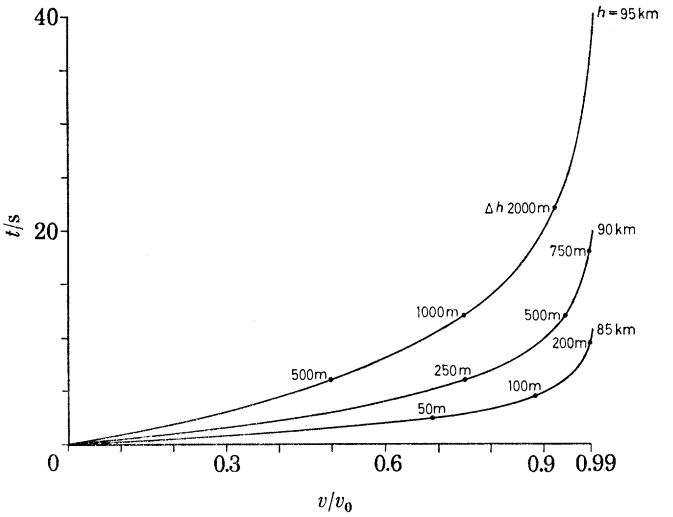

FIGURE 14. The behaviour of our chaff clouds in horizontal winds at different heights. The time which is necessary for the cloud to assume the fraction v/v_0 of a constant horizontal wind, which starts to blow at $t = 0$ is presented.

to the surrounding air. At that time a wind of a constant horizontal velocity v_0 starts to blow. The time which is necessary for the cloud to assume the fraction v/v_0 of the wind speed is presented, and the corresponding fall height differences are indicated on the different curves.

By comparing the experimental fall rates with C.I.R.A. 1965 data, $\rho(h)$ was approximated between 80 and 95 km by $\rho[\mathrm{kg\ m^{-3}}] = 4.05 \times 10^{-4}\ (v[\mathrm{m\ s^{-1}}])^{-1.32}$, where v is the vertical fall speed. Finally we tested the c_w approximation given by equation (1). From the investigations published by Hoerner (1965) it can be concluded that in the range of the Reynolds numbers concerned ($Re \approx 0.01 \ldots 1$), a really good approximation of c_w is

$$c_w = C(Re)^{-1} = C\frac{\eta}{v\rho l},$$

where the constant C is not well known for our chaff dipoles.

Now, in the height range of our measurements, the mean free path λ of the air molecules is comparable or greater than the width of the individual dipoles. In this case the viscosity η is given by

$$\eta = \frac{1}{3}\frac{\bar{u}\rho\lambda}{1+\lambda/l}$$

or, introducing $\lambda = a/\rho$, by

$$\eta = \frac{a}{3}\frac{\bar{u}\rho}{\rho + a/l}.$$

Substituting η into c_w and c_w into the equation of the equilibrium mentioned above one finds that in this case the fall rates should be

$$v_\perp = \text{const.} \left(\frac{1}{\rho} + \frac{l}{a}\right)$$

(ρ is supposed to be known from the C.I.R.A. 1965 data in the form of an exponential function of height with a constant (mean) scale height in the height range of our measurements).

In the case discussed above, the measured fall rates have been approximated in the limited height range between 83 and 95 km by an exponential function of height, the constant (mean) scale height of which was found by the experiment. If one now approximates v, given in the last equation, by a purely exponential function of height, in the same height range, the constant mean scale height of this approximation depends on l/a. (The mean exponential densities of air being known from C.I.R.A.) By selecting l/a such that our *experimental* mean scale heights of $v_\perp$ are fitted l/a is determined, and with the width l of our chaff diploes a is known.

By this procedure a was found to be $a \approx 1.1 \times 10^{-7}$ kg/m^2. From ρ and a the mean free paths of the molecules can be determined. They were estimated to be about 1 cm at $h = 83$ km and 9.1 cm at $h = 95$ km. Further a is determined theoretically by

$$a = \frac{1}{4\sqrt{2}\,\pi N r^2}$$

(N = (mean) specific number density, r (mean) molecule radius. In the height range under concern $N \approx 2.09 \times 10^{25}$ kg^{-1}, $r \approx 1.6 \times 10^{-10}$ m). With these values a is found to be

$$a \approx 1.04 \times 10^{-7} \text{ kg m}^{-2}.$$

The c_w values obtained above from the mean exponential fall rates do not differ by more than 4 % from those obtained by fitting the more accurate formula of the drag coefficient as far as heights between 84 and 94 km are concerned.

Mean air temperatures (figure 3) have been estimated by using the average scale heights of ρ as being deduced from the fall rates after their calibration. The slight dependence of viscosity on temperature has been neglected.

References (Rose *et al.*)

Bowhill, S. A. 1969 Ion chemistry of the D- and E-regions – a survey of working group 11 of the inter-union commission on solar-terrestrial physics. *J. atmos. terr. Phys.* **31**, 731–741.

Dieminger, W. 1952 Uber die Ursachen der exzessiven Absorption in der Ionosphäre an Wintertagen. *J. atmos. terr. Phys.* **2**, 340.

Dieminger, W., Rose, G. & Widdel, H. U. 1966 On the existence of anomalous radio wave absorption during winter in 40° northern latitude. *J. atmos. terr. Phys.* **28**, 317–318.

Gregory, J. B. & Manson, A. U. 1969 Seasonal variations of electron densities below 100 km at mid-latitudes. *J. atmos. terr. Phys.* **31**, 703–729.

Hoerner, S. F. 1965 *Fluid-dynamic drag*. Library of Congress Catalog Card Number 64–19666, USA, published by the author.

Manson, A. U. 1971 The concentration and transport of minor constituents in the mesosphere and lower thermosphere (70–100 km) during periods of 'anomalous absorption'. Preprint. (Institute of Space and Atmosph. Studies, University of Saskatchewan), to be published in *J. atmos. terr. Phys.*

Rose, G., Schubart, W., Weber, J., Widdel, H. U. & Galdon, P. 1971 Ergebnisse von Bodenmessungen der Kurzwellenabsorption in Spanien. *Kleinheubacher Berichte* **14**, 239–246.

Rose, G., Widdel, H. U., Azcárraga, A. & Sanchez, L. 1972 A payload for small sounding rockets for wind finding and density measurements in the height region between 95 and 75 km. *Phil. Trans. R. Soc. Lond.* A **271**, 509.

Weber, J. 1967 Nachweis der Winteranomalie von Kurzwellen in der Ionosphäre des europäischen Mittelmeerraumes. Diplomarbeit, Univ. Göttingen.

PHILOSOPHICAL TRANSACTIONS OF THE ROYAL SOCIETY A MATHEMATICAL, PHYSICAL & ENGINEERING SCIENCES

Discussion

R. A. Hamilton (*Meteorological Office, London Road, Bracknell, Berks*)

Observations have been quoted by Dr Widdel showing anomalous features during the period December 1969 to January 1970, so it may be useful to summarize very briefly the results of the meteorological rockets soundings at South Uist (57° N, 07° W) and at Kiruna (68° N, 20° E) during that period. The table below gives T the maximum temperature measured at the stratopause, in °C, and ρ the density at 60 km in 10^{-6} kg m^{-2} at these places on the dates shown.

When the sounding did not reach 60 km the value of ρ is obtained by extrapolation from the height given in parentheses.

Table

South Uist						Kiruna		
	T/°C	ρ/mg m^{-2}		T/°C	ρ/mg m^{-2}		T/°C	ρ/mg m^{-2}
2 Dec.	−2	168 (59)	1 Jan.	+19	306 (57)	7 Jan.	−19	232 (54)
4	+6	183	3	+15	299	9	−13	244
8	+13	190	6	−1	293	12	−9	274
11	+10	202	9	−1	266	19	−6	210
15	−4	169	12	+6	269	21	−2	217
17	0	180 (58)	14	+18	278	23	−10	230 (58)
19	+11	234	16	+18	299	26	+10	288
23	−4	217	26	+35	287	28	+16	310
27	+29	250 (56)	27	+35	277 (58)	30	+9	296
30	+30	301	29	+35	306			

PHILOSOPHICAL TRANSACTIONS OF THE ROYAL SOCIETY A MATHEMATICAL, PHYSICAL & ENGINEERING SCIENCES